



Persymmetric Adaptive Union Subspace Detection

Liyang Pan¹, Yongchan Gao^{1*}, Zhou Ye², Yuzhou Lv² and Ming Fang²

¹School of Electronic Engineering, Xidian University, Xi'an, China, ²Shanghai Aerospace Electronic Technology Institute, Shanghai, China

This paper addresses the detection of a signal belonging to several possible subspace models, namely, a union of subspaces (UoS), where the active subspace that generated the observed signal is unknown. By incorporating the persymmetric structure of received data, we propose three UoS detectors based on GLRT, Rao, and Wald criteria to alleviate the requirement of training data. In addition, the detection statistic and classification bound for the proposed detectors are derived. Monte-Carlo simulations demonstrate the detection and classification performance of the proposed detectors over the conventional detector in training-limited scenarios.

Keywords: adaptive detection, signal detection, subspace detection, persymmetry, union of subspaces

OPEN ACCESS

Edited by:

Chengpeng Hao,
Institute of Acoustics (CAS), China

Reviewed by:

Jian Kang,
Soochow University, China
Zhanye Chen,
Chongqing University, China
Pia Addabbo,
Giustino Fortunato University, Italy
Da Xu,
Institute of Acoustics (CAS), China

*Correspondence:

Yongchan Gao
ycgao@xidian.edu.cn

Specialty section:

This article was submitted to
Radar Signal Processing,
a section of the journal
Frontiers in Signal Processing

Received: 23 September 2021

Accepted: 05 November 2021

Published: 15 December 2021

Citation:

Pan L, Gao Y, Ye Z, Lv Y and Fang M
(2021) Persymmetric Adaptive Union
Subspace Detection.
Front. Sig. Proc. 1:782182.
doi: 10.3389/frsip.2021.782182

1 INTRODUCTION

Adaptive detection (Liu et al., 2021; Rong et al., 2021) of signals usually assumes a homogeneous environment, namely, the clutter in the cell under test is independent and identically distributed with the training data from adjacent cells. However, it is difficult to satisfy the homogeneity of the noise in practice due to power fluctuations. Among the possible non-homogeneous models, the partially homogeneous environment (PHE) is proven effective and widely used in radar signal detection (Pulsone and Raghavan, 1999; Bandiera et al., 2007), especially for the generalized likelihood ratio test (GLRT) and two-step GLRT (Conte et al., 2001), the adaptive cosine estimator (Kraut and Scharf, 1999), and the Rao and Wald tests (Gao et al., 2020). The PHE assumes the noise in the cell under test and the training data sharing the same covariance matrix but different power levels.

The detectors above only take rank-one signal into consideration, i.e., the nominal steering vector is in accordance with the actual steering vector. However, the actual array radar has model errors (De Maio, 2005; Yu et al., 2019) such as antenna pointing error, array element position error, and channel mismatch. In practical application, if the model error is not considered, the detection performance may be reduced greatly. Scharf and Friedlander (1994) and Kraut et al. (2001) assume that the target signal comes from a multi-rank subspace to illustrate the indeterminacy of the target steering vector. Besides, more specific subspace detectors for various detecting environments have been proposed (Liu et al., 2014; Gao et al., 2018; Mao et al., 2019). However, the data in many real-world scenarios tend to be generated by processes that switch/operate in different modes (Lodhi and Bajwa, 2018). In such instances, data generated through each mode of the process can be modeled as lying on a subspace, in which case the entire data generated during the process as a whole can be best described as coming from a union of subspaces. In recent years, UoS detection has been attracting many researchers' attention (Joneidi et al., 2015; Wimalajeewa et al., 2015). Based on the UoS model, Lodhi and Bajwa (2018) derived the bounds on the performances of UoS detector in terms of geometry of subspaces.

Although effective, the methods mentioned above fail to detect signals without sufficient training data. Real scenarios are generally training-limited due to the limitations of the environment and the radar system itself (Aubry et al., 2021; Aubry et al., 2018). The persymmetric structure of the

covariance matrix is considered to alleviate the requirement of training data. Persymmetric structure means that the noise covariance matrix is Hermitian about its principal diagonal and persymmetric about its cross diagonal, which often exists in a uniformly distributed linear array or uniformly pulse trains. Many methods considered the persymmetric structure in the design of detectors. For homogeneous environments, such typical detectors are persymmetric ACE (Gao et al., 2015), persymmetric AMF (Pailloux et al., 2011), persymmetric invariant test (Ciunzono et al., 2016), persymmetric Rao and Wald tests (Wang et al., 2016), persymmetric subspace Rao (Gao et al., 2019), and persymmetric subspace tunable detection method (Liu et al., 2018). For PHE, many detectors have been proposed in Hao et al. (2012), Liu et al. (2014), and Mao et al. (2019).

To the best of the authors' knowledge, the design of persymmetric union subspace signal detection in PHE has not been developed yet. In this paper, we address the detection of a signal belonging to several possible subspace models, namely, a union of subspaces in PHE. Not only did the active subspace of UoS generate the observed signal, but also the power scale is unknown. Based on GLRT, Rao, and Wald criteria, we exploit the persymmetric structure of received data in the design of detection, thus proposing three UoS detectors to alleviate the amount of training data. Besides, the detection statistic and classification bound for the proposed detectors are derived. Numerical results demonstrate the detection and classification performance of the proposed detectors in training-limited scenarios.

Notations: Vector and matrix are denoted by boldface lower case and upper case letters, respectively. $(\cdot)^*$, $(\cdot)^T$, and $(\cdot)^H$ denote complex conjugate, transpose, and complex conjugate transpose, respectively. The notation \sim denotes "be distributed as." $|\cdot|$ represents the determinant of a matrix, and $\text{tr}(\cdot)$ represents the trace of a matrix.

2 PROBLEM FORMULATION

In this section, we formulate the problem model of UoS detection. There are N pulses over a coherent processing interval (CPI). In this paper, we assume that the target signal $\mathbf{s} \in \mathbb{C}^{N \times 1}$ comes from a union of subspaces. Let K_0 different subspaces \mathbf{S}_k , $k = 1, \dots, K_0$ represent different characteristics of the target signal. Then, the target \mathbf{s} can be expressed by $\mathbf{s} = \mathbf{H}_k \boldsymbol{\alpha}_k$, $k = 1, \dots, K_0$, where $\mathbf{H}_k \in \mathbb{C}^{N \times q}$ denotes the k th subspace matrix, and $\boldsymbol{\alpha}_k$ the corresponding coordinate.

The collected test data are modeled as $\mathbf{x} \in \mathbb{C}^{N \times 1}$. If a target signal is detected, the test data can be expressed by $\mathbf{x} = \mathbf{s} + \mathbf{n}$, where $\mathbf{n} \sim \mathcal{CN}(\mathbf{0}, \sigma^2 \mathbf{M})$ represents the clutter in a non-homogeneous environment, where σ^2 denotes the power scaling factor, and \mathbf{M} the covariance matrix of clutter. Thus, the UoS signal detection problem can be formulated by

$$\begin{aligned}
 H_0: & \begin{cases} \mathbf{x} = \mathbf{n}, \\ \mathbf{x}_p = \mathbf{n}_p, & p = 1, \dots, N_0; \end{cases} \\
 H_k: & \begin{cases} \mathbf{x} = \mathbf{s} + \mathbf{n}, & \mathbf{s} \in \mathbf{S}_k, k = 1, \dots, K_0 \\ \mathbf{x}_p = \mathbf{n}_p, & p = 1, \dots, N_0; \end{cases} \quad (1)
 \end{aligned}$$

where \mathbf{x}_p , $p = 1, \dots, N_0$ denotes the training data collected from adjacent range cells of the test data, which contain clutter $\mathbf{n}_p \sim \mathcal{CN}(\mathbf{0}, \mathbf{M})$, $p = 1, \dots, N_0$ only. Moreover, the detection problem can be formulated as two hypotheses: the null hypothesis H_0 indicating that there is no target signal in the observation, and an alternative hypothesis H_k (Lodhi and Bajwa, 2018) representing that a UoS signal is detected. In traditional signal detection, the target signal can be seen as belonging to a low-dimensional subspace. In contrast, our purpose is to detect the UoS signal, so we assume the case of the target signal \mathbf{s} belonging to a union of low-dimensional subspaces: $\mathbf{s} \in \cup_{k=1}^{K_0} \mathbf{S}_k$, and this is referred to as the detection stage. After detecting the UoS signal, we deal with the problem of active subspace detection, whose goal is to identify the subspace \mathbf{S}_k to which \mathbf{s} belongs, and this stage is referred to as the classification stage.

3 THE PROPOSED PERSYMMETRIC UOS DETECTORS

In this section, we exploit the persymmetric structure to propose three UoS detectors, by resorting to GLRT, Rao, and Wald criteria.

First, a unitary matrix is used to transform the collected data and the assumed UoS matrix, where the unitary matrix is denoted as

$$\mathbf{T} = \begin{cases} \frac{1}{\sqrt{2}} \begin{bmatrix} \mathbf{I}_{N/2} & \mathbf{J}_{N/2} \\ j\mathbf{I}_{N/2} & -j\mathbf{J}_{N/2} \end{bmatrix} & \text{for } N \text{ even,} \\ \frac{1}{\sqrt{2}} \begin{bmatrix} \mathbf{I}_{(N-1)/2} & \mathbf{0} & \mathbf{J}_{(N-1)/2} \\ \mathbf{0} & \sqrt{2} & \mathbf{0} \\ j\mathbf{I}_{(N-1)/2} & \mathbf{0} & -j\mathbf{J}_{(N-1)/2} \end{bmatrix} & \text{for } N \text{ odd.} \end{cases} \quad (2)$$

where \mathbf{J} denotes the permutation matrix.

The transforming process can be formulated by

$$\begin{aligned}
 \tilde{\mathbf{x}} &= \mathbf{T}\mathbf{x}, \tilde{\mathbf{x}}_p = \mathbf{T}\mathbf{x}_p, \tilde{\mathbf{H}}_k = \mathbf{T}\mathbf{H}_k, \\
 \tilde{\mathbf{n}} &= \mathbf{T}\mathbf{n}, \tilde{\mathbf{n}}_p = \mathbf{T}\mathbf{n}_p, \mathbf{R} = \mathbf{T}\mathbf{M}\mathbf{T}^H. \quad (3)
 \end{aligned}$$

It is worth noting that \mathbf{R} denotes a real symmetric matrix. Thus, the detection problem in Eq. 1 is rewritten as:

$$\begin{aligned}
 H_0: & \begin{cases} \tilde{\mathbf{x}} = \tilde{\mathbf{n}}, \\ \tilde{\mathbf{x}}_p = \tilde{\mathbf{n}}_p, & p = 1, \dots, N_0; \end{cases} \\
 H_k: & \begin{cases} \tilde{\mathbf{x}} = \tilde{\mathbf{s}} + \tilde{\mathbf{n}}, & \tilde{\mathbf{s}} \in \tilde{\mathbf{S}}_k, k = 1, \dots, K_0 \\ \tilde{\mathbf{x}}_p = \tilde{\mathbf{n}}_p, & p = 1, \dots, N_0; \end{cases} \quad (4)
 \end{aligned}$$

3.1 P-UoS-GLRT Detector Design

The GLRT detector can be formulated by

$$\frac{\max_{\sigma^2} \max_{\boldsymbol{\alpha}_k} f_1(\tilde{\mathbf{x}}) H_k}{\max_{\sigma^2} f_0(\tilde{\mathbf{x}}) H_0} \geq \gamma, \quad (5)$$

where $f_1(\tilde{\mathbf{x}})$ denotes the probability density function (pdf) of $\tilde{\mathbf{x}}$ under the alternative hypothesis, and $f_0(\tilde{\mathbf{x}})$ represents the pdf of $\tilde{\mathbf{x}}$ under hypothesis H_0 . These two statistics can be expressed as follows:

$$f_1(\tilde{\mathbf{x}}) = \frac{1}{\pi^N \sigma^{2N} |\mathbf{R}|} \exp\left[-(\tilde{\mathbf{x}} - \tilde{\mathbf{H}}_k \boldsymbol{\alpha}_k)^H \mathbf{R}^{-1} (\tilde{\mathbf{x}} - \tilde{\mathbf{H}}_k \boldsymbol{\alpha}_k) / \sigma^2\right] \quad (6)$$

$$f_0(\tilde{\mathbf{x}}) = \frac{1}{\pi^N \sigma^{2N} |\mathbf{R}|} \exp[-\tilde{\mathbf{x}}^H \mathbf{R}^{-1} \tilde{\mathbf{x}} / \sigma^2] \quad (7)$$

To obtain the MLE (maximum likelihood estimation) of $\boldsymbol{\alpha}_k$, we can resort to the derivative of $f_1(\tilde{\mathbf{x}})$. Take the derivative of $f_1(\tilde{\mathbf{x}})$ with respect to $\boldsymbol{\alpha}_k$, and set the derivative equal to zero, then the estimation of $\boldsymbol{\alpha}_k$ is obtained:

$$\hat{\boldsymbol{\alpha}}_k = \arg \max_{\boldsymbol{\alpha}_k} f_1(\tilde{\mathbf{x}}) = \left(\tilde{\mathbf{H}}_k^H \mathbf{R}^{-1} \tilde{\mathbf{H}}_k\right)^{-1} \tilde{\mathbf{H}}_k^H \mathbf{R}^{-1} \tilde{\mathbf{x}} \quad (8)$$

To solve the problem shown in Eq. 5, the MLE of σ^2 is supposed to be obtained as follows:

$$\hat{\sigma}_1^2 = \left[\tilde{\mathbf{x}}^H \mathbf{R}^{-1} \tilde{\mathbf{x}} - \tilde{\mathbf{x}}^H \mathbf{R}^{-1} \tilde{\mathbf{H}}_k \left(\tilde{\mathbf{H}}_k^H \mathbf{R}^{-1} \tilde{\mathbf{H}}_k\right)^{-1} \tilde{\mathbf{H}}_k^H \mathbf{R}^{-1} \tilde{\mathbf{x}}\right] / N \quad (9)$$

$$\hat{\sigma}_0^2 = (\tilde{\mathbf{x}}^H \mathbf{R}^{-1} \tilde{\mathbf{x}}) / N \quad (10)$$

Substitute Eqs 8–10 into the GLRT detector Eq. 5 to obtain the rewritten expression of GLRT:

$$\frac{\tilde{\mathbf{x}}^H \mathbf{R}^{-1} \tilde{\mathbf{x}}}{\tilde{\mathbf{x}}^H \mathbf{R}^{-1} \tilde{\mathbf{x}} - \tilde{\mathbf{x}}^H \mathbf{R}^{-1} \tilde{\mathbf{H}}_k \left(\tilde{\mathbf{H}}_k^H \mathbf{R}^{-1} \tilde{\mathbf{H}}_k\right)^{-1} \tilde{\mathbf{H}}_k^H \mathbf{R}^{-1} \tilde{\mathbf{x}}} \geq \gamma \quad H_k / H_0 \quad (11)$$

Obtain the MLE of \mathbf{R} by using the training data and transform it into a symmetric one:

$$\hat{\mathbf{R}} = \frac{1}{N_0} \sum_{p=1}^{N_0} \mathbf{x}_p \mathbf{x}_p^H \quad (12)$$

$$\hat{\mathbf{R}}_p = \mathbf{T}^H \hat{\mathbf{R}} \mathbf{T} \quad (13)$$

Replace \mathbf{R} in Eq. 11 with $\hat{\mathbf{R}}_p$, obtaining

$$\frac{\tilde{\mathbf{x}}^H \hat{\mathbf{R}}_p^{-1} \tilde{\mathbf{x}}}{\tilde{\mathbf{x}}^H \hat{\mathbf{R}}_p^{-1} \tilde{\mathbf{x}} - \tilde{\mathbf{x}}^H \hat{\mathbf{R}}_p^{-1} \tilde{\mathbf{H}}_k \left(\tilde{\mathbf{H}}_k^H \hat{\mathbf{R}}_p^{-1} \tilde{\mathbf{H}}_k\right)^{-1} \tilde{\mathbf{H}}_k^H \hat{\mathbf{R}}_p^{-1} \tilde{\mathbf{x}}} \geq \gamma \quad H_k / H_0 \quad (14)$$

Let $\mathbf{P}_{\tilde{\mathbf{H}}_k} = \tilde{\mathbf{H}}_k \left(\tilde{\mathbf{H}}_k^H \hat{\mathbf{R}}_p^{-1} \tilde{\mathbf{H}}_k\right)^{-1} \tilde{\mathbf{H}}_k^H \hat{\mathbf{R}}_p^{-1}$ denote the projection matrix of $\tilde{\mathbf{H}}_k$. Then, Eq. 14 can be rewritten as

$$\frac{\tilde{\mathbf{x}}^H \hat{\mathbf{R}}_p^{-1} \tilde{\mathbf{x}}}{\tilde{\mathbf{x}}^H \hat{\mathbf{R}}_p^{-1} \tilde{\mathbf{x}} - \tilde{\mathbf{x}}^H \hat{\mathbf{R}}_p^{-1} \mathbf{P}_{\tilde{\mathbf{H}}_k} \tilde{\mathbf{x}}} \geq \gamma \quad H_k / H_0 \quad (15)$$

Let \hat{k} be the index of the maximum value of the GLRT test Eq. 15, then the P-UoS-GLRT detector can be formulated by

$$\frac{\tilde{\mathbf{x}}^H \hat{\mathbf{R}}_{\hat{k}}^{-1} \tilde{\mathbf{x}}}{\tilde{\mathbf{x}}^H \hat{\mathbf{R}}_{\hat{k}}^{-1} \tilde{\mathbf{x}} - \tilde{\mathbf{x}}^H \hat{\mathbf{R}}_{\hat{k}}^{-1} \mathbf{P}_{\tilde{\mathbf{H}}_{\hat{k}}} \tilde{\mathbf{x}}} \geq \gamma \quad H_k / H_0 \quad (16)$$

In order to examine the performance of classification, we have to resort to classification probability bounds, as the exact expressions could not be acquired directly, and the target should be identified in a specific subspace in the UoS. Let $g(\tilde{\mathbf{x}}, \tilde{\mathbf{H}}_k) = \tilde{\mathbf{x}}^H \hat{\mathbf{R}}_p^{-1} \mathbf{P}_{\tilde{\mathbf{H}}_k} \tilde{\mathbf{x}}$, $h(\tilde{\mathbf{x}}) = \tilde{\mathbf{x}}^H \hat{\mathbf{R}}_p^{-1} \tilde{\mathbf{x}}$, then the classification probability bound of the P-UoS-GLRT test can be expressed by

$$P_{H_k}(\tilde{H}_k) \geq \max \left\{ 0, P_{S_k} \left(\frac{h(\tilde{\mathbf{x}})}{h(\tilde{\mathbf{x}}) - g(\tilde{\mathbf{x}}, \tilde{\mathbf{H}}_k)} > \gamma \right) + \sum_{j=1, j \neq k}^{K_0} P_{S_k} \left(\frac{h(\tilde{\mathbf{x}}) - g(\tilde{\mathbf{x}}, \tilde{\mathbf{H}}_k)}{h(\tilde{\mathbf{x}}) - g(\tilde{\mathbf{x}}, \tilde{\mathbf{H}}_j)} > 1 \right) - (K_0 - 1) \right\} \quad (17)$$

3.2 P-UoS-Rao Detector Design

Assume that the unknown parameters $\boldsymbol{\theta} = [\boldsymbol{\theta}_r^T, \theta_s]^T$, where $\boldsymbol{\theta}_r = \boldsymbol{\alpha}_k$ stands for the corresponding coordinate, $\theta_s = \sigma^2$ represents the power scaling factor which is deterministic but known, and \mathbf{R} is known. Thus, the Rao test is formulated by

$$\frac{\partial \ln f_1(\tilde{\mathbf{x}}|\boldsymbol{\theta})}{\partial \boldsymbol{\theta}_r} \bigg|_{\boldsymbol{\theta}=\hat{\boldsymbol{\theta}}_0} \left[\mathbf{J}^{-1}(\hat{\boldsymbol{\theta}}_0) \right]_{\boldsymbol{\theta}_r, \boldsymbol{\theta}_r} \frac{\partial \ln f_1(\tilde{\mathbf{x}}|\boldsymbol{\theta})}{\partial \boldsymbol{\theta}_r^*} \bigg|_{\boldsymbol{\theta}=\hat{\boldsymbol{\theta}}_0} \geq \xi, \quad H_k / H_0 \quad (18)$$

where $\mathbf{J}(\boldsymbol{\theta})$ is a Fisher information matrix which is given by

$$\mathbf{J}(\boldsymbol{\theta}) = \begin{bmatrix} \mathbf{J}_{\boldsymbol{\theta}_r, \boldsymbol{\theta}_r} & \mathbf{J}_{\boldsymbol{\theta}_r, \theta_s} \\ \mathbf{J}_{\boldsymbol{\theta}_s, \boldsymbol{\theta}_r} & \mathbf{J}_{\boldsymbol{\theta}_s, \theta_s} \end{bmatrix}, \quad (19)$$

and

$$[\mathbf{J}^{-1}(\boldsymbol{\theta})]_{\boldsymbol{\theta}_r, \boldsymbol{\theta}_r} = [\mathbf{J}_{\boldsymbol{\theta}_r, \boldsymbol{\theta}_r}(\boldsymbol{\theta}) - \mathbf{J}_{\boldsymbol{\theta}_r, \theta_s}(\boldsymbol{\theta}) \mathbf{J}_{\boldsymbol{\theta}_s, \theta_s}^{-1}(\boldsymbol{\theta}) \mathbf{J}_{\boldsymbol{\theta}_s, \boldsymbol{\theta}_r}(\boldsymbol{\theta})]^{-1} \quad (20)$$

$\hat{\boldsymbol{\theta}}_0 = [\hat{\boldsymbol{\theta}}_{r,0}^T, \hat{\theta}_{s,0}]^T$ denotes the MLE of $\boldsymbol{\theta}$ under null hypothesis H_0 . The pdf of $\tilde{\mathbf{x}}$ under the alternative hypothesis is given by

$$f_1(\tilde{\mathbf{x}}|\boldsymbol{\theta}) = \frac{1}{(\pi \sigma^2)^N |\mathbf{R}|} \exp \left[-\frac{(\tilde{\mathbf{x}} - \tilde{\mathbf{H}}_k \boldsymbol{\alpha}_k)^H \mathbf{R}^{-1} (\tilde{\mathbf{x}} - \tilde{\mathbf{H}}_k \boldsymbol{\alpha}_k)}{\sigma^2} \right]. \quad (21)$$

The Fisher information matrix is expressed as follows:

$$\mathbf{J}(\boldsymbol{\theta}) = \mathbb{E} \left\{ \left[\frac{\partial \ln f_1(\tilde{\mathbf{x}}|\boldsymbol{\theta})}{\partial \boldsymbol{\theta}^*} \right] \left[\frac{\partial \ln f_1(\tilde{\mathbf{x}}|\boldsymbol{\theta})}{\partial \boldsymbol{\theta}^T} \right] \right\}. \quad (22)$$

It is straightforward to obtain the derivative

$$\frac{\partial \ln f_1(\tilde{\mathbf{x}}|\boldsymbol{\theta})}{\partial \boldsymbol{\theta}_r} = \frac{2}{\sigma^2} \left[(\tilde{\mathbf{x}} - \tilde{\mathbf{H}}_k \boldsymbol{\alpha}_k)^H \mathbf{R}^{-1} \tilde{\mathbf{H}}_k \right]^T, \quad (23)$$

$$\frac{\partial \ln f_1(\tilde{\mathbf{x}}|\boldsymbol{\theta})}{\partial \boldsymbol{\theta}_r^*} = \frac{2}{\sigma^2} \left[\tilde{\mathbf{H}}_k^H \mathbf{R}^{-1} (\tilde{\mathbf{x}} - \tilde{\mathbf{H}}_k \boldsymbol{\alpha}_k) \right]. \quad (24)$$

Thus, the $\mathbf{J}_{\boldsymbol{\theta}_r, \boldsymbol{\theta}_r}(\boldsymbol{\theta})$ under H_0 can be obtained as follows:

$$\mathbf{J}_{\boldsymbol{\theta}_r, \boldsymbol{\theta}_r}(\boldsymbol{\theta}_0) = \frac{4}{\sigma^2} \tilde{\mathbf{H}}_k^H \mathbf{R}^{-1} \tilde{\mathbf{H}}_k. \quad (25)$$

Since $\mathbf{J}_{\boldsymbol{\theta}_r, \theta_s}(\boldsymbol{\theta})$ is a null matrix, we can obtain

$$[\mathbf{J}^{-1}(\boldsymbol{\theta}_0)]_{\boldsymbol{\theta}_r, \boldsymbol{\theta}_r} = \mathbf{J}_{\boldsymbol{\theta}_r, \boldsymbol{\theta}_r}^{-1}(\boldsymbol{\theta}_0) = \frac{\sigma^2}{4} \left(\tilde{\mathbf{H}}_k^H \mathbf{R}^{-1} \tilde{\mathbf{H}}_k \right)^{-1} \quad (26)$$

Substituting Eqs. 23, 24, and 26 into the Rao test Eq. 18, the rewritten expression of Rao can be formulated as

$$\frac{\tilde{\mathbf{x}}^H \mathbf{R}^{-1} \tilde{\mathbf{H}}_k \left(\tilde{\mathbf{H}}_k^H \mathbf{R}^{-1} \tilde{\mathbf{H}}_k \right)^{-1} \tilde{\mathbf{H}}_k^H \mathbf{R}^{-1} \tilde{\mathbf{x}} H_k}{\sigma^2} \underset{H_0}{\geq} \lambda \quad (27)$$

Next, the MLE of σ^2 under H_0 is obtained as follows:

$$\hat{\theta}_{s,0} = \hat{\sigma}_0^2 = \arg \max_{\sigma^2} f_0(\tilde{\mathbf{x}}|\theta) = \tilde{\mathbf{x}}^H \mathbf{R}^{-1} \tilde{\mathbf{x}}/N \quad (28)$$

where $f_0(\tilde{\mathbf{x}}|\theta)$ denotes the pdf of $\tilde{\mathbf{x}}$ under H_0 , which can be expressed by

$$f_0(\tilde{\mathbf{x}}|\theta) = \frac{1}{\pi^N \sigma^{2N} |\mathbf{R}|} \exp\left(-\frac{\tilde{\mathbf{x}}^H \mathbf{R}^{-1} \tilde{\mathbf{x}}}{\sigma^2}\right) \quad (29)$$

Substituting it into Eq. 27, the Rao test can be rewritten as

$$\frac{\tilde{\mathbf{x}}^H \mathbf{R}^{-1} \tilde{\mathbf{H}}_k \left(\tilde{\mathbf{H}}_k^H \mathbf{R}^{-1} \tilde{\mathbf{H}}_k \right)^{-1} \tilde{\mathbf{H}}_k^H \mathbf{R}^{-1} \tilde{\mathbf{x}} H_k}{\tilde{\mathbf{x}}^H \mathbf{R}^{-1} \tilde{\mathbf{x}}} \underset{H_0}{\geq} \lambda \quad (30)$$

Replacing \mathbf{R} by its symmetric MLE $\hat{\mathbf{R}}_p$, the P-UoS-Rao detector can be formulated as

$$\frac{\tilde{\mathbf{x}}^H \hat{\mathbf{R}}_p^{-1} \tilde{\mathbf{H}}_k \left(\tilde{\mathbf{H}}_k^H \hat{\mathbf{R}}_p^{-1} \tilde{\mathbf{H}}_k \right)^{-1} \tilde{\mathbf{H}}_k^H \hat{\mathbf{R}}_p^{-1} \tilde{\mathbf{x}} H_k}{\tilde{\mathbf{x}}^H \hat{\mathbf{R}}_p^{-1} \tilde{\mathbf{x}}} \underset{H_0}{\geq} \lambda, \quad (31)$$

which equals

$$\frac{\tilde{\mathbf{x}}^H \hat{\mathbf{R}}_p^{-1} \mathbf{P}_{\tilde{\mathbf{H}}_k} \tilde{\mathbf{x}} H_k}{\tilde{\mathbf{x}}^H \hat{\mathbf{R}}_p^{-1} \tilde{\mathbf{x}}} \underset{H_0}{\geq} \lambda \quad (32)$$

Let \hat{k} be the index of the maximum value of the Rao test Eq. 32, then the P-UoS-Rao detector can be formulated by

$$\frac{\tilde{\mathbf{x}}^H \hat{\mathbf{R}}_p^{-1} \mathbf{P}_{\tilde{\mathbf{H}}_{\hat{k}}} \tilde{\mathbf{x}} H_k}{\tilde{\mathbf{x}}^H \hat{\mathbf{R}}_p^{-1} \tilde{\mathbf{x}}} \underset{H_0}{\geq} \lambda \quad (33)$$

Finally, the classification probability bound of the P-UoS-Rao detector can be derived as

$$P_{H_k}(\tilde{H}_k) \geq \max \left\{ 0, P_{S_k} \left(\frac{g(\tilde{\mathbf{x}}, \tilde{\mathbf{H}}_k)}{h(\tilde{\mathbf{x}})} > \gamma \right) + \sum_{j=1, j \neq k}^{K_0} P_{S_k} \left(\frac{g(\tilde{\mathbf{x}}, \tilde{\mathbf{H}}_k)}{g(\tilde{\mathbf{x}}, \tilde{\mathbf{H}}_j)} > 1 \right) - (K_0 - 1) \right\} \quad (34)$$

3.3 P-UoS-Wald Detector Design

The Wald test is formulated by

$$\left(\hat{\theta}_{r,1} - \theta_{r,0} \right)^H \left\{ \left[\mathbf{J}^{-1}(\hat{\theta}_1) \right]_{\theta_r, \theta_r} \right\}^{-1} \left(\hat{\theta}_{r,1} - \theta_{r,0} \right) \underset{H_0}{\geq} \xi. \quad (35)$$

where $\theta_{r,1}$ denotes the coordinate α_k under the alternative hypothesis.

From $f_1(\tilde{\mathbf{x}}|\theta)$ denoted in Eq. 21, we can obtain the MLE of $\theta_{r,1}$,

$$\begin{aligned} \hat{\theta}_{r,1} &= \arg \max_{\alpha_k} f_1(\tilde{\mathbf{x}}|\theta) \\ &= \left(\tilde{\mathbf{H}}_k^H \mathbf{R}^{-1} \tilde{\mathbf{H}}_k \right)^{-1} \tilde{\mathbf{H}}_k^H \mathbf{R}^{-1} \tilde{\mathbf{x}}, \end{aligned} \quad (36)$$

and $\theta_{r,0} = \mathbf{0}_{q \times 1}$. According to Eq. 22, $\mathbf{J}_{\theta_r, \theta_r}(\hat{\theta})$ under the alternative hypothesis is given by

$$\mathbf{J}_{\theta_r, \theta_r}(\hat{\theta}_1) = \frac{4}{\sigma^2} \tilde{\mathbf{H}}_k^H \mathbf{R}^{-1} \tilde{\mathbf{H}}_k. \quad (37)$$

Since $\mathbf{J}_{\theta_r, \theta_r}(\hat{\theta}_1)$ is a null matrix, it is straightforward that

$$\left[\mathbf{J}^{-1}(\hat{\theta}_1) \right]_{\theta_r, \theta_r} = \mathbf{J}_{\theta_r, \theta_r}^{-1}(\hat{\theta}_1) = \frac{\sigma^2}{4} \left(\tilde{\mathbf{H}}_k^H \mathbf{R}^{-1} \tilde{\mathbf{H}}_k \right)^{-1}. \quad (38)$$

Substituting Eqs. 36, 38 into the Wald test Eq. 35, the rewritten expression of Wald can be formulated by

$$\frac{\tilde{\mathbf{x}}^H \mathbf{R}^{-1} \tilde{\mathbf{H}}_k \left(\tilde{\mathbf{H}}_k^H \mathbf{R}^{-1} \tilde{\mathbf{H}}_k \right)^{-1} \tilde{\mathbf{H}}_k^H \mathbf{R}^{-1} \tilde{\mathbf{x}} H_k}{\sigma^2} \underset{H_0}{\geq} \xi \quad (39)$$

The MLE of σ^2 under the alternative hypothesis is expressed as follows:

$$\begin{aligned} \hat{\theta}_{s,1} &= \hat{\sigma}_1^2 \\ &= \arg \max_{\sigma^2} f_1(\tilde{\mathbf{x}}|\theta) \end{aligned} \quad (40)$$

$$= \frac{1}{N} \left[\tilde{\mathbf{x}}^H \mathbf{R}^{-1} \tilde{\mathbf{x}} - \tilde{\mathbf{x}}^H \mathbf{R}^{-1} \tilde{\mathbf{H}}_k \left(\tilde{\mathbf{H}}_k^H \mathbf{R}^{-1} \tilde{\mathbf{H}}_k \right)^{-1} \tilde{\mathbf{H}}_k^H \mathbf{R}^{-1} \tilde{\mathbf{x}} \right]$$

Moreover, by replacing σ^2 in Eq. 39 by $\hat{\theta}_{s,1}$, Eq. 39 could be rewritten as

$$\frac{\tilde{\mathbf{x}}^H \mathbf{R}^{-1} \tilde{\mathbf{H}}_k \left(\tilde{\mathbf{H}}_k^H \mathbf{R}^{-1} \tilde{\mathbf{H}}_k \right)^{-1} \tilde{\mathbf{H}}_k^H \mathbf{R}^{-1} \tilde{\mathbf{x}} H_k}{\tilde{\mathbf{x}}^H \mathbf{R}^{-1} \tilde{\mathbf{x}} - \tilde{\mathbf{x}}^H \mathbf{R}^{-1} \tilde{\mathbf{H}}_k \left(\tilde{\mathbf{H}}_k^H \mathbf{R}^{-1} \tilde{\mathbf{H}}_k \right)^{-1} \tilde{\mathbf{H}}_k^H \mathbf{R}^{-1} \tilde{\mathbf{x}} H_0} \underset{H_0}{\geq} \xi \quad (41)$$

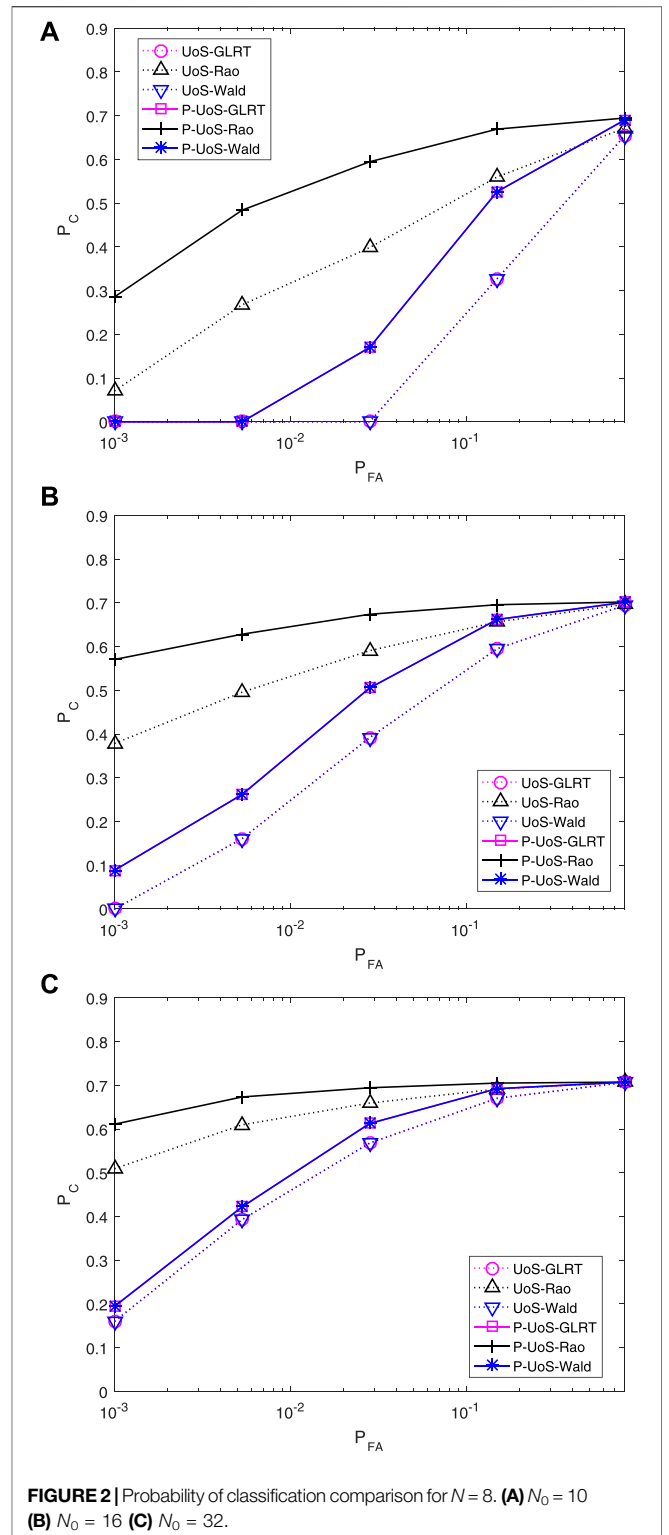
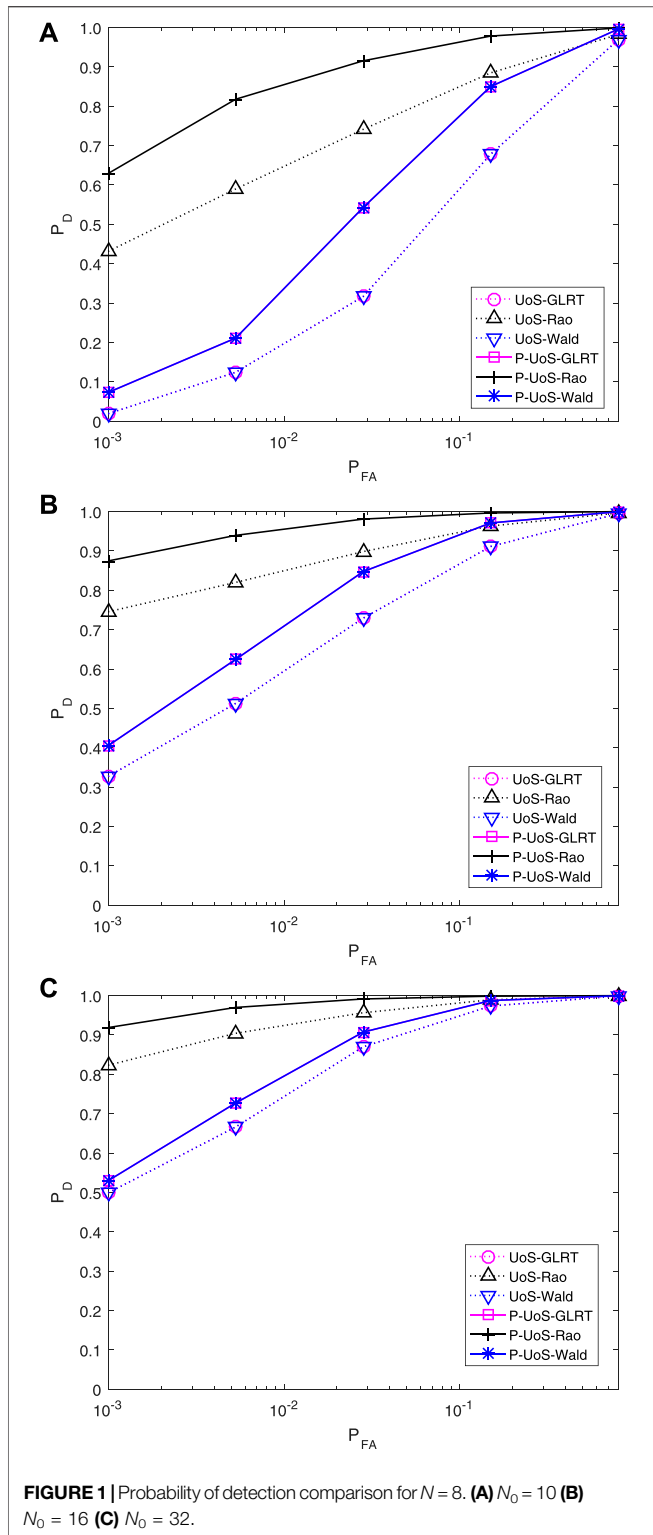
Substitute Eq. 13 into Eq. 41, then obtain the P-UoS-Wald detector

$$\frac{\tilde{\mathbf{x}}^H \hat{\mathbf{R}}_p^{-1} \mathbf{P}_{\tilde{\mathbf{H}}_{\hat{k}}} \tilde{\mathbf{x}} H_k}{\tilde{\mathbf{x}}^H \hat{\mathbf{R}}_p^{-1} \tilde{\mathbf{x}} - \tilde{\mathbf{x}}^H \hat{\mathbf{R}}_p^{-1} \mathbf{P}_{\tilde{\mathbf{H}}_{\hat{k}}} \tilde{\mathbf{x}} H_0} \underset{H_0}{\geq} \xi \quad (42)$$

Let \hat{k} be the index of the maximum value of the Wald test Eq. 42, then the P-UoS-Wald detector can be formulated by

$$\frac{\tilde{\mathbf{x}}^H \hat{\mathbf{R}}_p^{-1} \mathbf{P}_{\tilde{\mathbf{H}}_{\hat{k}}} \tilde{\mathbf{x}} H_k}{\tilde{\mathbf{x}}^H \hat{\mathbf{R}}_p^{-1} \tilde{\mathbf{x}} - \tilde{\mathbf{x}}^H \hat{\mathbf{R}}_p^{-1} \mathbf{P}_{\tilde{\mathbf{H}}_{\hat{k}}} \tilde{\mathbf{x}} H_0} \underset{H_0}{\geq} \xi \quad (43)$$

Finally, the classification probability bound of P-UoS-Wald can be derived by



$$P_{H_k}(\tilde{H}_k) \geq \max \left\{ 0, P_{S_k} \left(\frac{g(\tilde{\mathbf{x}}, \tilde{\mathbf{H}}_k)}{h(\tilde{\mathbf{x}}) - g(\tilde{\mathbf{x}}, \tilde{\mathbf{H}}_k)} > \gamma \right) + \sum_{j=1, j \neq k}^{K_0} P_{S_k} \left(\frac{g(\tilde{\mathbf{x}}, \tilde{\mathbf{H}}_k)(h(\tilde{\mathbf{x}}) - g(\tilde{\mathbf{x}}, \tilde{\mathbf{H}}_j))}{g(\tilde{\mathbf{x}}, \tilde{\mathbf{H}}_j)(h(\tilde{\mathbf{x}}) - g(\tilde{\mathbf{x}}, \tilde{\mathbf{H}}_k))} > 1 \right) - (K_0 - 1) \right\} \quad (44)$$

4 NUMERICAL RESULT

In this section, numerical results are provided to illustrate the detection and classification performance of the proposed detectors named P-UoS-GLRT, P-UoS-Rao, and P-UoS-Wald over the traditional ones [UoS-GLRT, UoS-Rao, and UoS-Wald (Pan et al., 2021)].

We use 10^4 Monte Carlo trials to evaluate the threshold and the probability of detection and classification. If not otherwise specified, we set $N = 8$, $\rho = 0.9$, $\sigma^2 = 0.7$, SNR = 10dB, the Doppler frequency $f_d = [0.09, 0.1]$, and the number of training data $N_0 = 10, 16, 32$, respectively, throughout this paper. For each false alarm probability P_{FA} , the statistics of detectors in each trial of the Monte Carlo experiment can be obtained. Arrange these statistics in descending order, then the threshold is the last statistic that occupies the preceding false alarm probability of all statistics. The detection probability and classification probability can be obtained by comparing the statistics obtained by using the observation with the threshold.

Figure 1 shows the detection performance of the proposed detectors and the traditional ones. It could be seen that as P_{FA} grows, the detection probability of detectors is improved remarkably, among which Rao has the highest detection probability and the GLRT detector shows the same performance with Wald. Moreover, with the increase in the number of samples, the detection performance is improved to some extent. As we can see in **Figure 1C**, among the proposed detectors, P-UoS-Rao has the best detection performance, followed by P-UoS-Rao and P-UoS-Wald, but all these three detectors perform better than their corresponding traditional ones. However, when the number of training data turns small, as is shown in **Figures 1A,B**, the detection probability of traditional detectors degrades greatly because of the lack of training data. However, the proposed persymmetric ones still keep high detection probability, exceeding the traditional ones greatly. Thus, the proposed persymmetric detectors have better detection performance in general environment, also in training-limited scenarios.

Similar results are shown in **Figure 2**. **Figure 2** plots the classification performance of the proposed detectors and the traditional ones. As we can see, the Rao detector has the highest classification probability, followed by the GLRT detector and the Wald detector. **Figure 2C** shows that P-UoS-Rao outperforms P-UoS-GLRT and P-UoS-Wald, and these three detectors all perform better over their corresponding traditional ones. By comparing **Figures 2A,B**, we can conclude that the proposed persymmetric detectors have higher classification probability, in both training-sufficient and training-limited scenarios.

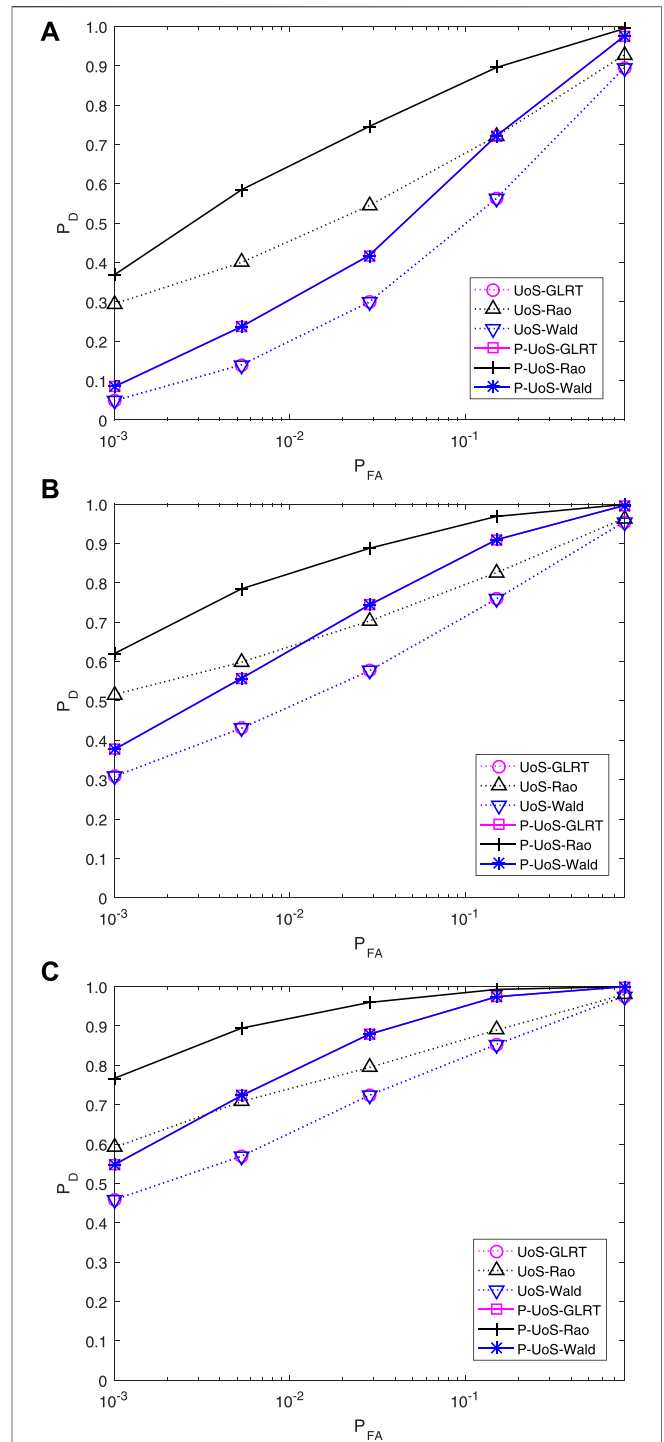
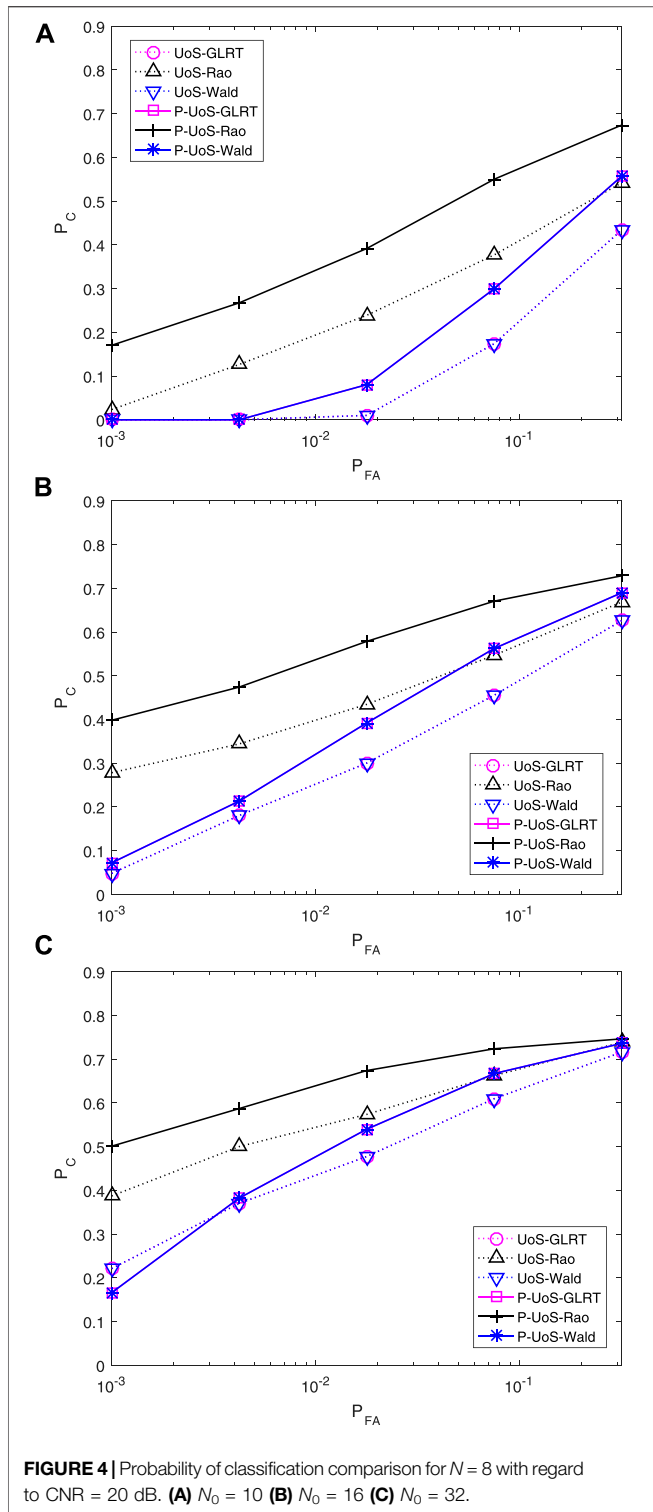
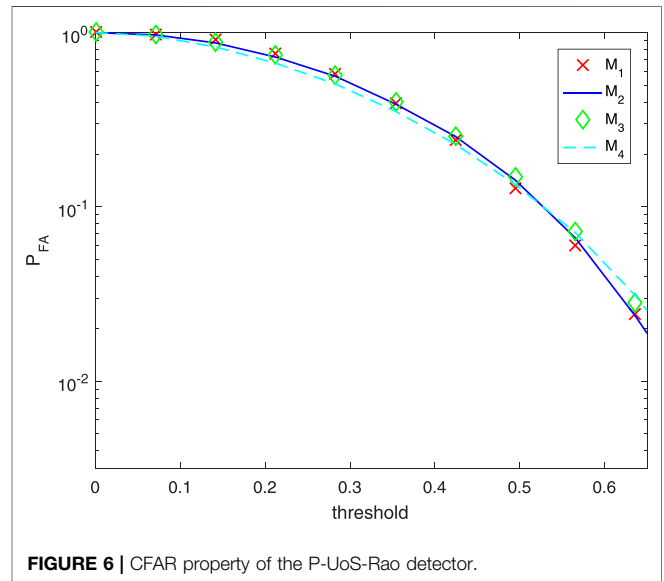
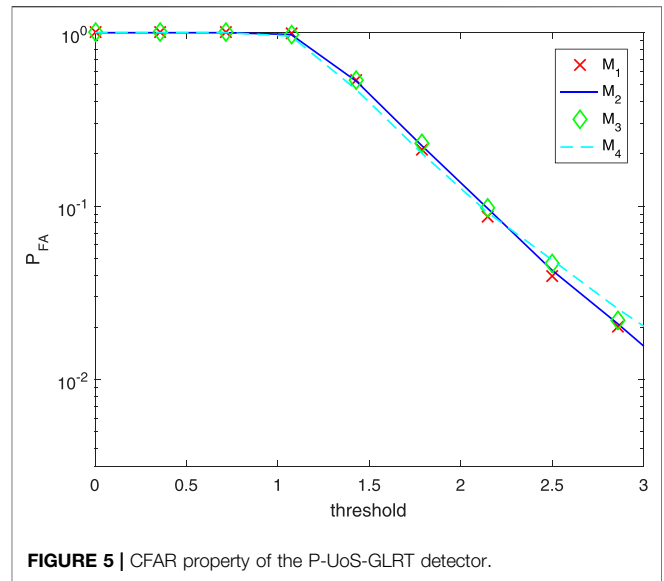


FIGURE 3 | Probability of detection comparison for $N = 8$ with regard to CNR = 20 dB. **(A)** $N_0 = 10$ **(B)** $N_0 = 16$ **(C)** $N_0 = 32$.

To better simulate the real detection scenario, the interference model containing clutter and noise is supposed to be considered. In the numerical experiment, we set CNR = 20dB and SNR = 20dB and evaluate the detection and classification performance of the proposed detectors, compared with the traditional ones. **Figure 3**

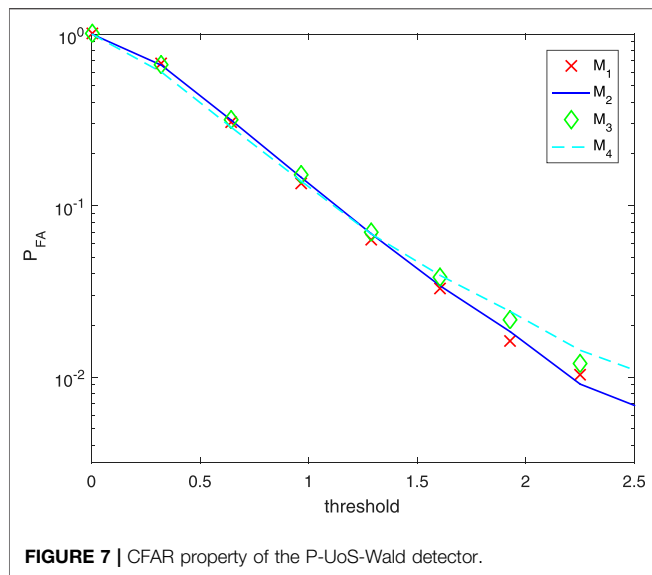


shows the detection probability of the proposed detectors and the traditional ones. Numerical results illustrate that the proposed persymmetric detectors outperform the traditional ones in signal detection both in the training-sufficient and in the training-limited scenarios. Among them, P-UoS-Rao has the best detection



performance, followed by P-UoS-GLRT and P-UoS-Wald, which is consistent with Figure 1. Figure 4 shows the classification probability of the proposed detectors. Moreover, the same simulation results with Figure 2 can be obtained; that is, the classification probability of the proposed persymmetric UoS detectors is higher than the traditional ones, both with sufficient training data and with limited training data.

Figures 5–7 show the CFAR property of the proposed detectors P-UoS-GLRT, P-UoS-Rao, and P-UoS-Wald, respectively. Each experiment of these three are under four kinds of interference covariance matrix with different clutters, among which M_1 represents $0.1^{|i-j|}$, M_2 denotes $0.5^{|i-j|}$, M_3 denotes $0.9^{|i-j|}$, and M_4 stands for $0.5^{(i-j)^2} e^{-j2\pi \cdot 0.2(i-j)} + 0.9^{-(i-j)^2} + \delta_{i,j}$. It can be seen that the P_{FA} under each of the four kinds of interference covariance matrix



approximately coincides with others, for all these three persymmetric UoS detectors. This demonstrates that the proposed detectors have an approximate CFAR property.

5 CONCLUSION

In this paper, we dealt with the detection of a signal that belonged to a union of subspaces in PHE. Not only did the active subspace of UoS generate the observed signal, but also the power scale is unknown. Based on the GLRT, Rao, and Wald criteria, we used the persymmetric structure of received data to design three UoS detectors to alleviate the amount of training data. Besides, the

REFERENCES

- Aubry, A., De Maio, A., and Pallotta, L. (2018). A Geometric Approach to Covariance Matrix Estimation and its Applications to Radar Problems. *IEEE Trans. Signal. Process.* 66, 907–922. doi:10.1109/TSP.2017.2757913
- Aubry, A., Maio, A. D., Marano, S., and Rosamilia, M. (2021). Structured Covariance Matrix Estimation with Missing-Data for Radar Applications via Expectation-Maximization. *IEEE Trans. Signal Process* 69, 5920–5934. doi:10.1109/TSP.2021.3111587
- Bandiera, F., De Maio, A., Greco, A. S., and Ricci, G. (2007). Adaptive Radar Detection of Distributed Targets in Homogeneous and Partially Homogeneous Noise Plus Subspace Interference. *IEEE Trans. Signal. Process.* 55, 1223–1237. doi:10.1109/tsp.2006.888065
- Ciuonzo, D., Orlando, D., and Pallotta, L. (2016). On the Maximal Invariant Statistic for Adaptive Radar Detection in Partially Homogeneous Disturbance with Persymmetric Covariance. *IEEE Signal. Process. Lett.* 23, 1830–1834. doi:10.1109/LSP.2016.2618619
- Conte, E., De Maio, A., and Ricci, G. (2001). GLRT-based Adaptive Detection Algorithms for Range-Spread Targets. *IEEE Trans. Signal. Process.* 49, 1336–1348. doi:10.1109/78.928688
- De Maio, A. (2005). Robust Adaptive Radar Detection in the Presence of Steering Vector Mismatches. *IEEE Trans. Aerosp. Electron. Syst.* 41, 1322–1337. doi:10.1109/TAES.2005.1561887
- Gao, Y., Ji, H., and Liu, W. (2019). Persymmetric Adaptive Subspace Detectors for Range-Spread Targets. *Digital Signal. Process.* 89, 116–123. doi:10.1016/j.dsp.2019.03.007

detection statistic and classification bound for the proposed detectors were derived. Numerical results demonstrated the detection and classification performance of the proposed detectors over its competitor, especially in training-limited scenarios.

DATA AVAILABILITY STATEMENT

The raw/processed data required to reproduce these findings cannot be shared at this time as the data also forms part of an ongoing study.

AUTHOR CONTRIBUTIONS

LP completed the simulation and main body of the paper. YG provided the idea and some writing part of the paper. ZY, YL, and MF completed some writing part and revision of the paper.

FUNDING

This work was supported by the China Postdoctoral Science Foundation under Grant 2020T130493 and 2019M653561, by the National Defense Science and Technology Foundation of China under Grant 2019-JCJQ-JJ-060, by the Aeronautical Foundation of China under Grant 20180181001, by the Aerospace Science and Technology Fund under Grant SAST 2018-098, and by the Natural Science Foundation of Shaanxi Province under Grant 2019JM-032.

- Gao, Y., Li, H., and Himed, B. (2018). Adaptive Subspace Tests for Multichannel Signal Detection in Auto-Regressive Disturbance. *IEEE Trans. Signal. Process.* 66, 5577–5587. doi:10.1109/TSP.2018.2869123
- Gao, Y., Liao, G., Zhu, S., and Yang, D. (2015). Generalised Persymmetric Parametric Adaptive Coherence Estimator for Multichannel Adaptive Signal Detection. *IET Radar, Sonar & Navigation* 9, 550–558. doi:10.1049/iet-rsn.2014.0101
- Gao, Y., Mao, L., Ji, H., and Pan, L. (2020). “Persymmetric Subspace Rao and Wald Tests for Distributed Target in Partially Homogeneous Environment,” in 2020 IEEE 11th Sensor Array and Multichannel Signal Processing Workshop (SAM), Hangzhou, China, June 8, 2020, 1–5. doi:10.1109/SAM48682.2020.9104407
- Hao, C., Orlando, D., Ma, X., and Hou, C. (2012). Persymmetric Rao and Wald Tests for Partially Homogeneous Environment. *IEEE Signal. Process. Lett.* 19, 587–590. doi:10.1109/LSP.2012.2207891
- Joneidi, M., Ahmadi, P., Sadeghi, M., and Rahnavard, N. (2015). Union of Low-Rank Subspaces Detector. *IET Signal. Process.* 10, 55–62. doi:10.1049/iet-spr.2015.0009
- Kraut, S., Scharf, L. L., and McWhorter, L. T. (2001). Adaptive Subspace Detectors. *IEEE Trans. Signal. Process.* 49, 1–16. doi:10.1109/78.890324
- Kraut, S., and Scharf, L. L. (1999). The CFAR Adaptive Subspace Detector Is a Scale-Invariant GLRT. *IEEE Trans. Signal. Process.* 47, 2538–2541. doi:10.1109/78.782198
- Liu, J., Liu, W., Gao, Y., Zhou, S., and Xia, X.-G. (2018). Persymmetric Adaptive Detection of Subspace Signals: Algorithms and Performance Analysis. *IEEE Trans. Signal. Process.* 66, 6124–6136. doi:10.1109/TSP.2018.2875416

- Liu, W., Liu, J., Hao, C., Gao, Y., and Wang, Y. L. (2021). Multichannel Adaptive Signal Detection: Basic Theory and Literature Review. *Science China. Inf. Sci.* doi:10.1007/s11432-020-3211-8
- Liu, W., Xie, W., Liu, J., and Wang, Y. (2014). Adaptive Double Subspace Signal Detection in Gaussian Background-Part I: Homogeneous Environments. *IEEE Trans. Signal. Process.* 62, 2345–2357. doi:10.1109/TSP.2014.2309556
- Lodhi, M. A., and Bajwa, W. U. (2018). Detection Theory for union of Subspaces. *IEEE Trans. Signal. Process.* 66, 6347–6362. doi:10.1109/TSP.2018.2875897
- Mao, L., Gao, Y., Yan, S., and Xu, L. (2019). Persymmetric Subspace Detection in Structured Interference and Non-homogeneous Disturbance. *IEEE Signal. Process. Lett.* 26, 928–932. doi:10.1109/LSP.2019.2913332
- Pailloux, G., Forster, P., Ovarlez, J.-P., and Pascal, F. (2011). Persymmetric Adaptive Radar Detectors. *IEEE Trans. Aerosp. Electron. Syst.* 47, 2376–2390. doi:10.1109/TAES.2011.6034639
- Pan, L., Gao, Y., Li, J., and Xin, Z. (2021). “Union of Subspaces Signal Detection and Classification Based on Rao and Wald Test,” in International Conference on Frontiers of Electronics, Information and Computation Technologies, Changsha, China, May 21, 2021, 1–6.
- Pulsone, N. B., and Raghavan, R. S. (1999). Analysis of an Adaptive CFAR Detector in Non-gaussian Interference. *IEEE Trans. Aerosp. Electron. Syst.* 35, 903–916. doi:10.1109/7.784060
- Rong, Y., Aubry, A., De Maio, A., and Tang, M. (2021). Adaptive Radar Detection in Low-Rank Heterogeneous Clutter via Invariance Theory. *IEEE Trans. Signal. Process.* 69, 1492–1506. doi:10.1109/TSP.2021.3058447
- Scharf, L. L., and Friedlander, B. (1994). Matched Subspace Detectors. *IEEE Trans. Signal. Process.* 42, 2146–2157. doi:10.1109/78.301849
- Wang, Z., Li, M., Chen, H., Lu, Y., Cao, R., Zhang, P., et al. (2016). Persymmetric Detectors of Distributed Targets in Partially Homogeneous Disturbance. *Signal. Process.* 128, 382–388. doi:10.1016/j.sigpro.2016.05.010
- Wimalajeewa, T., Eldar, Y. C., and Varshney, P. K. (2015). Subspace Recovery from Structured union of Subspaces. *IEEE Trans. Inform. Theor.* 61, 2101–2114. doi:10.1109/TIT.2015.2403260
- Yu, X., Cui, G., Kong, L., Li, J., and Gui, G. (2019). Constrained Waveform Design for Colocated MIMO Radar with Uncertain Steering Matrices. *IEEE Trans. Aerosp. Electron. Syst.* 55, 356–370. doi:10.1109/TAES.2018.2852200

Conflict of Interest: The authors declare that the research was conducted in the absence of any commercial or financial relationships that could be construed as a potential conflict of interest.

Publisher’s Note: All claims expressed in this article are solely those of the authors and do not necessarily represent those of their affiliated organizations, or those of the publisher, the editors, and the reviewers. Any product that may be evaluated in this article, or claim that may be made by its manufacturer, is not guaranteed or endorsed by the publisher.

Copyright © 2021 Pan, Gao, Ye, Lv and Fang. This is an open-access article distributed under the terms of the Creative Commons Attribution License (CC BY). The use, distribution or reproduction in other forums is permitted, provided the original author(s) and the copyright owner(s) are credited and that the original publication in this journal is cited, in accordance with accepted academic practice. No use, distribution or reproduction is permitted which does not comply with these terms.